

## Electrical conductivity of long-range-ordered alloys

J. BANHART<sup>1</sup> and G. CZYCHOLL<sup>2</sup>

<sup>1</sup> *Hahn-Meitner-Institute - Glienicker Str. 100, 14109 Berlin, Germany*

<sup>2</sup> *Institute for Theoretical Physics, University of Bremen - 28359 Bremen, Germany*

(received 15 June 2001; accepted in final form 23 January 2002)

PACS. 72.15.Eb – Electrical and thermal conduction in crystalline metals and alloys.

**Abstract.** – The electrical resistivity of disordered, partially ordered and long-range-ordered gold-copper alloys was calculated from first principles by applying the coherent-potential approximation (CPA) and the Kubo-Greenwood equation to lattices with 2 or 4 atoms per unit cell and varying the occupation probabilities within each cell. In a first step the composition-dependent resistivity for disordered alloys and alloys with the highest possible degree of order was calculated for the entire composition range. After this the experimental resistivity as a function of composition was modelled by calculating the resistivity based on reasonable values for the concentration-dependent order parameter and using lattice structures determined from the phase diagram for each concentration. The experimental resistivity for annealed alloys with its pronounced minima for the two stoichiometric compositions could be perfectly reproduced.

*Introduction.* – The electrical resistivity of alloys is extremely sensitive to atomic rearrangements or structural changes of any kind. A striking example can be found in many textbooks: the resistivity of gold-copper alloys varies smoothly with concentration whenever Au and Cu atoms are distributed randomly on an fcc lattice, whereas some pronounced minima are found when the atom species are allowed to form an ordered arrangement. The corresponding data from ref. [2] are displayed in fig. 1 together with some results to be discussed later. The behaviour of the resistivity can easily be understood in a qualitative way: electrical resistivity is created by deviations from translational symmetry which are very pronounced in the disordered state. Ordering brings an alloy quite close to a translationally invariant configuration in which there is hardly any impurity scattering and resistivity is therefore small. Despite the seemingly simple physics of the phenomenon, a quantitative description is still lacking. Beside some simple models (see, *e.g.*, [4]) no successful attempts to calculate the effect of ordering on the electrical resistivity of alloys are known of. In this letter we provide an adequate formalism for calculating these effects in a parameter-free way — “from first principles” — and apply it to the alloy gold-copper. Au-Cu is attractive because it is one of the most intensively studied alloys and because it exhibits at least two different low-temperature ordered phases, namely the cubic AuCu<sub>3</sub> (L1<sub>2</sub>) structure and the tetragonal AuCuI (L1<sub>0</sub>) structure (fig. 2).

*Method.* – The starting point for the calculations is a theoretical scheme developed for disordered alloys, namely an approach which starts from a *local density functional* description

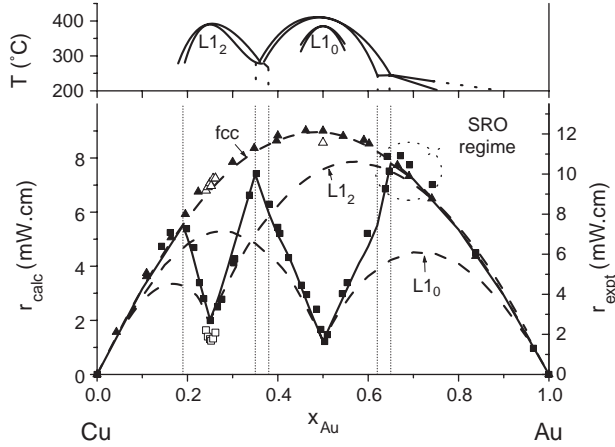


Fig. 1 – Top: part of the phase diagram of Au-Cu [1]. Bottom: electrical resistivity for disordered and ordered Au-Cu alloys. Full symbols: experimental values at  $T = 300$  K [2] extrapolated to  $T = 0$  K by subtracting the averaged resistivity of the pure components  $x\rho_{\text{Au}} + (1-x)\rho_{\text{Cu}}$  (triangles: quenched from above  $T_c =$  disordered, squares: annealed = ordered). Open symbols: experimental values measured at  $T = 21$  K [3]. Broken line: calculated resistivity for disordered fcc alloys and for  $L_{12}$  or  $L_{10}$  superstructures with reduced order (based on curves 2 in fig. 3). Full line: calculated composite resistivity using order parameters given by curves 3 in fig. 3. The vertical lines mark the compositions which separate different regimes (see table II). Note that calculated resistivities are enlarged by 35% in comparison to experimental values.

of the many-particle problem, treats disorder in the framework of the *coherent potential approximation* (CPA) in conjunction with the *Korringa-Kohn-Rostoker* (KKR) method and uses the rigorous *Kubo-Greenwood formula* of linear-response theory for the transport calculation. This has led to excellent results for the conductivity of paramagnetic [5–7] and ferromagnetic alloys [8] and even for optical properties [9].

Although the CPA deals with totally disordered systems, it can be used to describe homogeneous long-range order. Consider the ordered  $\text{AuCu}_3$  structure ( $L_{12}$ ) shown in fig. 2. It can be viewed as a simple cubic lattice with a basis of 4 atoms. Denote the probability for finding a gold atom on the  $i$ -th site of the basis  $x_i$  ( $i = 1, \dots, 4$ ). Complete disorder corresponds to  $x_i = 0.25$  for all  $i$ . One could treat this case by applying the KKR-CPA to a complex lattice with 4 atoms per unit cell and searching for 4 effective scatterers which represent on the average all possible occupations of the 4-atom basis with appropriate statistical weights [10]. Of course all four scatterers are identical in the case of disorder and the problem is equivalent to the much more simple task of searching for one effective scatterer on an fcc lattice. By choosing non-equal  $x_i$ , however, one can move away from disorder. One extreme case corresponds to total order. Here one sublattice is occupied exclusively by Au atoms, while the remaining positions are Cu sites, *i.e.*  $x_1 = 1$  and  $x_2 = x_3 = x_4 = 0$  using the numbering defined in fig. 2. As there is only one possible configuration in this case the averaging procedure is trivial and the effective scatterers are just the pure components Au and Cu. Partially ordered states can be obtained by choosing occupation values between these limits. In such cases the KKR-CPA is a non-trivial problem and one has to solve the full set of KKR-CPA equations to obtain 4 non-equal effective scatterers.

The ordered phase  $\text{AuCuI}$  ( $L_{10}$ ) can be treated in an analogous way. The structure consists of alternating planes in an fcc lattice exclusively occupied either by Au or by Cu. We use a

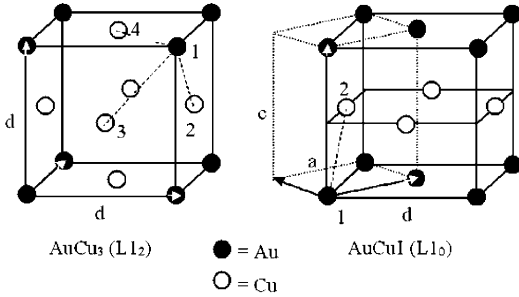


Fig. 2

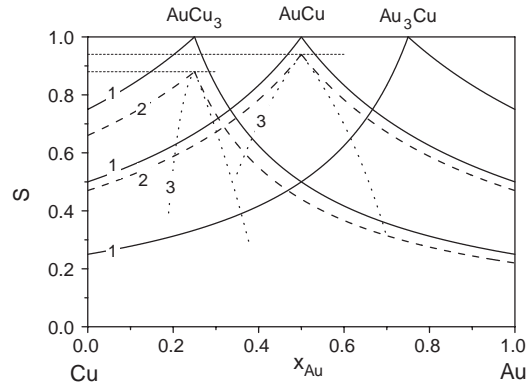


Fig. 3

Fig. 2 – Two of the ordered structures occurring in the Au-Cu system. Dashed lines connect the atoms of an individual unit cell, the vectors are the basis vectors of the respective structure.

Fig. 3 – Bragg-Williams order parameters  $S$  used in calculations. Curves 1: highest possible order parameter; curves 2: order reduced by choosing a non-zero auxiliary parameter  $\epsilon(x)$  which is  $\epsilon = 0.03$  (0.09) for stoichiometric  $L1_0$  ( $L1_2$ ) and drops to 0 linearly for  $x$  approaching 0 or 1; curves 3: same as 2 except that  $\epsilon(x)$  increases quadratically according to eq. (3). Horizontal broken lines: order parameter for  $L1_2$  and  $L1_0$  samples derived from experimental data.

tetragonal unit cell with a 2-atomic basis and tetragonal lattice constants  $a = d/\sqrt{2}$  and  $c = d$ , where  $d$  is the fcc lattice constant (see fig. 2, r.h.s.). A tetragonal distortion can be introduced to account for the experimentally known fact that  $c/d = 0.93$  in real AuCuI alloys [11]. In both cases disorder corresponds to  $x_1 = x_2 = 0.5$ , complete order to  $x_1 = 1$ ,  $x_2 = 0$  and partial order to values between these.

In off-stoichiometric alloys no perfect order can be achieved because the excess Au (Cu) has to be accommodated on Cu(Au) sites. The site occupations which correspond to the highest possible degree of order are given in table I. For this case the auxiliary parameter  $\epsilon$  which will be explained later has to be set to zero. From the lattice occupations  $x_i$  the familiar Bragg-Williams order parameter  $S$  can be derived which quantifies the fraction of Au (Cu) atoms correctly placed on a Cu(Au) sublattice [12]. The full line in fig. 3 shows  $S$  as a function of composition for the two superstructures considered.

The calculations were carried out in the following way: The KKR-CPA equations were first solved self-consistently for random fcc alloys using experimental lattice constants corresponding to the disordered state [11]. This way potentials for 40 alloys covering the entire composition range were obtained. These potentials and lattice constants were used in all the following calculations of both ordered and partially ordered states, *i.e.* the slight change in lattice constant upon ordering was ignored. Moreover, it was assumed that the potential is not very sensitive to the precise nature of the neighbourhood of an atom, *i.e.* that atomic potentials of the disordered state can be used for partially ordered alloys without introducing a significant error. While the validity of the former assumption could be verified explicitly by varying the lattice constant, the latter one is supported indirectly by calculations on other alloy systems beside Au-Cu which also yielded good results [13].

In a second step KKR-CPA calculations based on the two structures  $L1_2$  and  $L1_0$  and the given order parameters were carried out. The output of such calculations is the configurationally averaged CPA Green function  $\langle G \rangle_{\text{conf}}$ , which is used to calculate the isotropic dc

TABLE I – Occupations of sublattice sites for the two ordered structures investigated.  $S$  is the Bragg-Williams order parameter. “Au-sites” are all sites on sublattice 1, “Cu-sites” are the sites on sublattice 2 (AuCuI) or 2,3,4 (AuCu<sub>3</sub>).  $\epsilon > 0$  is an auxiliary parameter allowing to introduce additional disorder, with  $\epsilon = 0$  corresponding to the highest possible degree of order.

Structure	Au concentration $x$	Au sites	Cu sites	$S$
AuCu <sub>3</sub> (L1 <sub>2</sub> )	0–0.25	$4x - \epsilon$	$\frac{\epsilon}{3}$	$\frac{3x - \epsilon}{4x(1 - x)}$
	0.25–1	$1 - \epsilon$	$\frac{1}{3}(4x - 1 + \epsilon)$	$\frac{1 - x - \epsilon}{4x(1 - x)}$
AuCuI (L1 <sub>0</sub> )	0–0.5	$2x - \epsilon$	$\epsilon$	$\frac{x - \epsilon}{2x(1 - x)}$
	0.5–1	$1 - \epsilon$	$2x - 1 + \epsilon$	$\frac{1 - x - \epsilon}{2x(1 - x)}$

conductivity by means of the Kubo-Greenwood equation [7, 14]:

$$\sigma = \frac{1}{3} \sum_{\mu=1}^3 \frac{\hbar}{V\pi} \text{Tr} \langle \text{Im} G(\epsilon_F) j_{\mu} \text{Im} G(\epsilon_F) j_{\mu} \rangle_{\text{conf}}. \quad (1)$$

Here  $j_{\mu}$  are the electronic current operators in the direction  $\mu$  and  $V$  the atomic volume. It is shown in ref. [14] how this expression can be evaluated in the framework of the KKR-CPA by expressing the average over the product of Green functions in terms of  $\langle G \rangle_{\text{conf}}$  and approximately evaluating the vertex corrections. All the Brillouin zones were sampled with about 70000 points. A density functional provided by Moruzzi *et al.* was used [15].

*Results.* – In a first set of calculations the resistivity was calculated for the entire composition range for each of the structures defined, namely disordered fcc and L1<sub>2</sub> or L1<sub>0</sub> with the highest possible degree of order (fig. 4). The resistivity of the disordered fcc phase exhibits

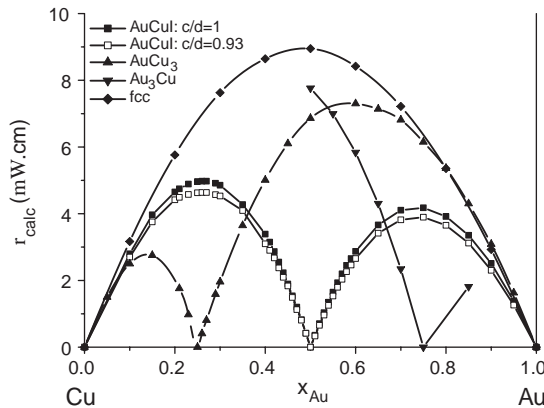


Fig. 4 – Calculated electrical resistivity for Au-Cu alloys. Diamonds: disordered fcc alloys, triangles: alloys with L1<sub>2</sub> (AuCu<sub>3</sub> structure), inverted triangles: hypothetical alloys with L1<sub>2</sub> (Au<sub>3</sub>Cu structure), squares: alloys with L1<sub>0</sub> structure based on  $c/d = 0.93$  (open) and 1 (closed). For all ordered superstructures the highest possible order parameter given by curve 1 in fig. 3 was used.

the familiar inverted parabola shape (“Nordheim’s rule”). The calculated resistivity is about 35% lower than the experimental data extrapolated to  $T = 0$  (given in fig. 1). Such deviations are often observed in calculations of this kind [7,8] and are a consequence of representing the real alloy with a complex atomic configuration containing lattice distortions, imperfections, impurities etc. by a muffin-tin alloy with only two different potential types on an otherwise perfect crystal lattice.

The resistivity curves for the two ordered superstructures show two inverted parabolae separated by zero resistivity for the perfectly ordered stoichiometric compositions. For all other compositions the resistivity is non-zero because the order parameter is smaller than 1. One can easily understand these curves if one thinks of the alloys as pseudobinary systems, *i.e.* AuCu<sub>3</sub> can be considered a binary Cu/AuCu<sub>3</sub> for  $x \leq 0.25$  and AuCu<sub>3</sub>/Au for  $x \geq 0.25$ , and AuCuI as Cu/AuCuI for  $x \leq 0.5$  or AuCuI/Au for  $x \geq 0.5$ . Assuming  $c/d = 0.93$  instead of  $c = d$  for the L1<sub>0</sub> structure does hardly change the resistivity. Therefore the influence of the tetragonal distortion due to the difference in atomic radii of Au and Cu is minute. Figure 4 also shows that the resistivity for the Au<sub>3</sub>Cu structure (which is the same as AuCu<sub>3</sub> with the atom species exchanged) behaves very similar to that of AuCu<sub>3</sub>. As there is no experimental evidence for this phase this is of more academic interest.

A second calculation was aimed at reproducing the resistivity of the actual alloy system with some of its phase complexity, *i.e.* the well-known curve known from the literature [2] given in fig. 1 (full squares). For the disordered phase the values already shown in fig. 4 can be taken. We plot experimental and theoretical resistivities on two scales in fig. 1 which differ by 35% to eliminate the difference between the two which was already mentioned and to make comparison easier. For ordered alloys a complete description is only possible if one makes additional assumptions and uses some adjustable parameters. The theory used in this paper exclusively treats resistivity caused by scattering at static impurities, whereas the experimental data [2] were obtained at room temperature and therefore contain significant contributions due to thermal scattering, leading to a quite large residual resistivity already for the pure elements. In order to eliminate some of the thermal effects, the simplest approach is to consider the line between the pure metal resistivities as base line and to subtract it from the experimental values. However, the corrected experimental values displayed in fig. 1 still show some thermal scattering for the ordered state as one can see from comparison with the few low-temperature measurements available. This is due to the known order dependence of the temperature effect [16]. Furthermore, even at the lowest temperatures the resistivities for the ordered compositions do not vanish as even extremely long annealing times do not yield perfect ordering because of the limited atomic mobility in the solid [17]. This residual disorder depends very much on the specific sample and cannot be predicted. We therefore take experimental values  $\rho(S)/\rho_0$  for the two ordered superstructures from ref. [2] and convert them into residual order parameters  $S_{\text{res}}$  by using Rossiter’s formula [12]:

$$\frac{\rho(S)}{\rho_0} = \frac{1 - S^2}{1 - AS^2}, \quad (2)$$

where  $\rho_0$  is the resistivity for random alloys ( $S = 0$ ). Further calculations and experiments suggest that the parameter  $A$  is between 0.3 [13],  $0.35 \pm 0.05$  [18] and 0.5 [17]. Using our value  $A = 0.3$  yields  $S_{\text{res}} = 0.88$  for the L1<sub>2</sub>,  $S_{\text{res}} = 0.94$  for the L1<sub>0</sub> samples used in ref. [2].

Disorder can be introduced into the model by deliberately misplacing atoms by adjusting the auxiliary parameter  $\epsilon$ . The expressions given in table I yield the required values for  $S$  if one assumes  $\epsilon = 0.09$  (0.03) for stoichiometric L1<sub>2</sub> (L1<sub>0</sub>). Further assuming that  $\epsilon(x)$  drops linearly to zero for  $x$  approaching the pure components, one obtains the composition-dependent order parameter shown in fig. 3 (curve 2). This choice for  $\epsilon(x)$  creates a nearly

TABLE II – *Partition of composition range of Au-Cu into segments corresponding to different phases as derived from phase diagram (fig. 1). Computational parameters used in modelling the experimental resistivity curve are given.*

Au concentration $x$	Structure	Computational parameters
$0 \leq 0.19$	random fcc	none
$0.19 \leq 0.35$	L1 <sub>2</sub>	$\epsilon_0 = 0.09, A = 64(16)$ for $x \leq (\geq) 0.25$
$0.35 \leq 0.38$	L1 <sub>2</sub> +L1 <sub>0</sub>	weighted average L1 <sub>2</sub> +L1 <sub>0</sub>
$0.38 \leq 0.62$	L1 <sub>0</sub>	$\epsilon_0 = 0.03, A = 3.5$ for all $x$
$0.62 \leq 0.65$	L1 <sub>0</sub> +fcc	weighted average L1 <sub>0</sub> +fcc
$0.65 \leq 1$	random fcc	none

composition-independent reduction of  $S$  compared to the state of maximum order (curve 1). The corresponding resistivities are given by broken lines in fig. 1 and are labelled “L1<sub>2</sub>” and “L1<sub>0</sub>”. Obviously, the minimum values of the experimental resistivity are well reproduced except, of course, for the 35% offset of the  $\rho$ -axes. The two curves are quite similar to the ones shown in fig. 4, the only difference being a small asymmetry and slightly higher maximum values due to the increased disorder. It is obvious that the experimental resistivity  $\rho(x)$  for off-stoichiometric compositions is not yet well described. Coming from the minima, the measured  $\rho(x)$  shows a nearly linear increase, whereas the calculations exhibit an inverted parabola. The reason for this could be twofold: firstly, the assumption of homogeneous disorder for non-stoichiometric compositions could be invalid. Excess gold or copper could segregate into clusters instead of uniformly populating the sublattices. Second, the assumption of a composition-independent disorder contribution to  $S$  could be unrealistic. The second reason can be assessed here: taking into account that the driving force for ordering is strongest for the ideal stoichiometric composition and falls off away from these compositions, it is reasonable to assume a concentration-dependent  $\epsilon(x)$  which has its minimum value  $\epsilon_0$  at  $x = 0.25$  or  $x = 0.5$  and increases for off-stoichiometric compositions. Good results were obtained by using the form

$$\epsilon(x) = \epsilon_0 + A(x - x_s)^2, \quad \text{for } x_s = 0.25 \quad \text{or } x_s = 0.5. \quad (3)$$

The choice of constants given in table II then yields curve 3 in fig. 3. Figure 1 shows the main result of this paper: a calculated composite resistivity curve obtained by dividing the entire concentration range into various segments, each one corresponding to a specific crystal structure determined from the experimental phase diagram. For each segment the resistivity was calculated using the respective structure and the parameters given in table II, after which the results were put together to the full line in fig. 1. The experimental values are very well represented by the resulting curve. The linear behaviour of  $\rho(x)$  on both sides of each stoichiometric composition can be reproduced perfectly. Only the region between 62 and 75 at.% Au is problematic, where in reality the alloy shows a more complicated phase composition than the assumed simple mix “L1<sub>0</sub>+fcc” or pure fcc. Moreover, the experimental finding that annealed samples have a higher resistivity than disordered alloys in this regime indicates that short-range order or other phenomena which are beyond the reach of the methods described in this paper could be important.

One should emphasise that in contrast to the calculations presented in the first part of this paper, this calculation is not parameter-free but uses a small number of phenomenological assumptions concerning the degree of residual order in the alloys which, however, are not

arbitrary but were derived directly from the experimental resistivity. Altogether, the excellent agreement of calculations and experiment is a great success of the alloy theory employed.

\* \* \*

We would like to thank H. EBERT and H. AKAI for providing some of their numerical routines for calculating structure constants and potentials.

#### REFERENCES

- [1] MASSALSKI T. B., *Binary Alloy Phase Diagrams* (American Society of Materials, Materials Park) 1983.
- [2] JOHANSSON C. H. and LINDE J. O., *Ann. Phys.*, **25** (1936) 1.
- [3] SEEMANN H. J., *Z. Phys.*, **62** (1930) 824.
- [4] CHRISTOPH V., RICHTER J. and SCHILLER W., *Phys. Status Solidi*, **100** (1980) 595.
- [5] SWIHART J. C., BUTLER W. H., STOCKS G. M., NICHOLSON D. M. and WARD R. C., *Phys. Rev. Lett.*, **57** (1986) 1181.
- [6] BROWN R. H., ALLEN P. B., NICHOLSON D. M. and BUTLER W. H., *Phys. Rev. Lett.*, **62** (1989) 661.
- [7] BANHART J., *Philos. Mag. B*, **77** (1998) 106.
- [8] BANHART J. and EBERT H., *Europhys. Lett.*, **32** (1995) 517.
- [9] BANHART J., *Phys. Rev. Lett.*, **82** (1999) 2139.
- [10] WEINBERGER P., *Electron Scattering Theory for Ordered and Disordered Matter* (Clarendon Press, Oxford) 1990.
- [11] PEARSON W. B., *A Handbook of Lattice Spacings and Structures of Metals and Alloys* (Pergamon, Oxford) 1958.
- [12] ROSSITER P. L., *The Electrical Resistivity of Metals and Alloys* (Cambridge University Press, Cambridge) 1987.
- [13] BANHART J. and CZYCHOLL G., unpublished work (2001).
- [14] BUTLER W. H., *Phys. Rev. B*, **31** (1985) 3260.
- [15] MORUZZI V. L., JANAK J. F. and WILLIAMS A. R., *Calculated Properties of Metals* (Pergamon Press, Oxford) 1978.
- [16] COLES B. R., *Physica*, **26** (1960) 143.
- [17] LANG H., UZAWA H., MOHRI T. and PFEILER W., *Intermetallics*, **9** (2001) 9.
- [18] SPRUŠIL B. and CHALUPA B., *Intermetallics*, **8** (2000) 831.